Coulomb Crystals

Thierry Matthey
Parallab
BCCS
University of Bergen
matthey@ii.uib.no

March 30, 2005

1 Paul Trap: General equation

A Coulom Cyrstal system consists of N ions with M different ion types. The ion type $i \in \{1, \ldots, M\}$ is defined by the mass m_i and the charge q_i, and $N = \sum_{i=1}^{M} N_i$. The system – based on Newton's Equation of Motion – is defined by a repulsive Coulombic part and a Paul Trap part trapping the ions to create a potential minimum in some spatial region. The linear Paul Trap potential with optional oscillating potential $(U_0, \vec{k})$ is defined by

$$U_{\text{pt}} = \sum_{i=1}^{N} \frac{1}{2} \left(m_i \left(\omega_{r_i} \left(1 + \frac{\alpha}{r_0^4} x_i^2 y_i^2 \right) \right)^2 (x_i^2 + y_i^2) + m_i \omega_{z_i}^2 z_i^2 \right) - U_0 k_B \cos(2\pi \vec{k} \cdot \vec{r_i}) \tag{1}$$

$$\omega_{r_j} = \sqrt{ (\omega_{r_1}^2 + \frac{1}{2}\omega_{z_1}^2) \left(\frac{q_j}{q_1} \frac{m_1}{m_j} \right)^2 - \frac{1}{2}\omega_{z_1}^2 \frac{q_j}{q_1} \frac{m_1}{m_j} } \tag{2}$$

$$\omega_{z_j} = \omega_{z_1} \sqrt{ \frac{q_j}{q_1} \frac{m_1}{m_j} } \tag{3}$$

$$\omega = \sqrt{ \frac{2\omega_r^2 + \omega_z^2}{3} } \tag{4}$$

$$U_{\text{coul}} = \sum_{i=1, j>i}^{N} \frac{q_i q_j}{||\vec{r_i} - \vec{r_j}||} \tag{5}$$

$$U = U_{\text{coul}} + U_{\text{pt}} \tag{6}$$

Here, ω_{r_j} and ω_{z_j} are the real ω's for ion type i in Eq. (1) derived from ω_{r_1} and ω_{z_1} of ion type 1 by Eqs. (2-3). $(x_i, y_i, z_i) = \vec{r_i}$ are coordinates; α and r_0 model the non-spherical part of Paul Trap. Note that in the equations above ω_{r_1} and ω_{z_1} do not have to be identical for the ion type with q_1 and m_1. The Wigner-Seitz radius is given by

$$a = \sqrt[3]{ \frac{Q^2}{k} } \tag{7}$$

$$Q^2 = \frac{2}{N(N-1)} \sum_{i=1}^{M} \left(q_i^2 \frac{N_i(N_i - 1)}{2} + \sum_{j=i+1}^{M} q_i q_j N_i N_j \right) \tag{8}$$

$$k = \frac{\sum_{i=1}^{N} m_i}{N} \omega^2 \tag{9}$$

Furthermore, the density n, the radius R of the Crystal, Q and k the effective charge and force constant, respectively, the equivalent energy of the homogeneous charge distribution U_{homo}, the cohesive (correlation or Madelung) energy U_{coh}, and Γ are related as following:

$$n = \frac{3}{4\pi a^3} = \frac{N}{V} \tag{10}$$

$$R = \sqrt[3]{\frac{NQ^2}{k}} = a\sqrt[3]{N} \tag{11}$$

$$U_{\text{homo}} = \frac{9}{10}\frac{Q^2}{a}N^{\frac{5}{3}} \tag{12}$$

$$U_{\text{coh}} = (U - U_{\text{homo}})\frac{a}{NQ^2} \tag{13}$$

$$\Gamma = \frac{Q^2}{ak_BT} \tag{14}$$

Cohesive energy for different packing:

$$U_{\text{coh}}^{\text{bcc}} = -0.895929255682 \tag{15}$$

$$U_{\text{coh}}^{\text{fcc}} = -0.895873615195 \tag{16}$$

$$U_{\text{coh}}^{\text{hcp}} = -0.895838120459 \tag{17}$$

Final structures, which have reached equillibrium, satisfy $U_{\text{coul}} = 2U_{\text{pt}}$.
The Mackay icosahedra system with M closed shells:

$$N = (2M + 1)(\frac{5}{3}M(M + 1) + 1) . \tag{18}$$

M	0	1	2	3	4	5	6	7	8	9
N	1	13	55	147	309	561	923	1415	2057	2869
M	10	11	12	13	14	15	16	17	18	19
N	3871	5083	6525	8217	10179	12431	14993	17885	21127	24739
M	20	21	22	23	24	25	26	27	28	29
N	28741	33153	37995	43287	49049	55301	62063	69355	77197	85609
M	30	31	32	33	34	35	36	37	38	39
N	94611	104223	114465	125357	136919	149171	162133	175825	190267	205479
M	40	41	42	43	44	45	46	47	48	49
N	221481	238293	255935	274427	293789	314041	335203	357295	380337	404349

2 Two-Componenet Wigner-Seitz Radius

We define the properties of a general mixed system with $N = N_1 + N_2$ ions, where N_i is the number of ions of type i. We make the *ansatz* that the Wigner-Seitz radius can be expressed in terms of effective charge Q and force constant k,

$$k = \frac{m_1 N_1 + m_2 N_2}{N}\omega^2, \tag{19}$$

and

$$Q^2 = \frac{q_1^2 N_1(N_1 - 1) + 2q_1 q_2 N_1 N_2 + q_2^2 N_2(N_2 - 1)}{N(N-1)}. \tag{20}$$

The effective Wigner-Seitz radius can then be expressed as

$$a = \left(\frac{q_1^2 N_1(N_1 - 1) + 2q_1 q_2 N_1 N_2 + q_2^2 N_2(N_2 - 1)}{(N-1)(m_1 N_1 + m_2 N_2)\omega^2}\right)^{1/3}. \tag{21}$$

We also note that in the limit of large N

$$\lim_{N\to\infty} a = \left(\frac{1}{N}\left(N_1\frac{q_1^2}{m_1\omega^2} + N_2\frac{q_2^2}{m_2\omega^2}\right)\right)^{1/3} = \left(\frac{1}{N}\left(N_1 a_1^3 + N_2 a_2^3\right)\right)^{1/3}. \tag{22}$$

Assuming a 50% mixture and equal charge-to-mass ratio, $q_2 = 2q_1$ and $m_2 = 2m_1$, Eqs. 19 and 20 become:

$$k = \frac{3}{2}m_1\omega^2 \text{ and } Q^2 = q_1^2\frac{9N - 10}{4(N-1)} \tag{23}$$

Finally, we can write the effective Wigner-Seitz radius as

$$a = \left(\frac{q_1^2}{m_1\omega^2}\frac{9N - 10}{6(N-1)}\right)^{1/3}, \tag{24}$$

$$\lim_{N\to\infty} a = \left(\frac{q_1^2}{m_1\omega^2}\frac{3}{2}\right)^{1/3} = a_1\left(\frac{3}{2}\right)^{1/3}. \tag{25}$$

3   2D cases with 3 Ca$^+$ and 2 A^{2+}

We studied a simple taste case with 3 Ca$^+$ and 2 A^{2+}, $\omega_r, \omega_z = 3 \cdot 10^{-9}$ [fs^{-1}] and four different masses to get an idea of how the ions arrange them self in equilibrium. We performed the simulation with PROTOMOL using leapfrog with NVT Nosé-Hoover thermostat.

A				**B**			
Type	Mass [amu]	Charge [e]	r [Å]	Type	Mass [amu]	Charge [e]	r [Å]
A	80.0	2.0	74504.9	A	160.0	2.0	59134.6
A	80.0	2.0	74504.9	A	160.0	2.0	59134.6
CA1	40.0	1.0	103013	CA1	80.0	1.0	81761.7
CA1	40.0	1.0	103013	CA1	80.0	1.0	81761.7
CA1	40.0	1.0	108136	CA1	80.0	1.0	85827.7
$\frac{103013}{74504.9} = 1.38263389387812$				$\frac{81761.7}{59134.6} = 1.38263723775928$			
C				**D**			
Type	Mass [amu]	Charge [e]	r [Å]	Type	Mass [amu]	Charge [e]	r [Å]
A	1600.0	2.0	27447.8	A	16000.0	2.0	12740.1
A	1600.0	2.0	27447.8	A	16000.0	2.0	12740.1
CA1	800.0	1.0	37950.4	CA1	8000.0	1.0	17615
CA1	800.0	1.0	37950.4	CA1	8000.0	1.0	17615
CA1	800.0	1.0	39837.7	CA1	8000.0	1.0	18491
$\frac{37950.4}{27447.8} = 1.38263904575230$				$\frac{17615}{12740.1} = 1.38264220845990$			

Table 1: 2D cases with 3 Ca$^+$ and 2 A^{2+}.

4 3D cases with 10 Ca_{40}^+ and 10 A_{80}^{2+}

We studied a simple taste case with 10 Ca^+ and 10 A^{2+}, $\omega_r, \omega_z = 2.5 \cdot 10^{-9}$ [fs^{-1}]. We performed the simulation of 10 [ms] with PROTOMOL using leapfrog with NVT Nosé-Hoover thermostat, $\delta t = 0.1$ [ns]. Table 2 shows the energy for different final configurations and the radii of the ions. It indicates that the most favorable configurations have one A_{80}^{2+} located at the origin.

Energy [kcal/mol]	Ca_{40}^+ radii, [μ m]		A_{80}^{2+} radii, [μ m]		Case
0.90462218		19.9115 - 20.2018	1.04571	18.2729 - 18.377	12
0.90462999		19.723 - 20.2261	2.06706	18.311 - 18.6596	03
0.90465249		19.6933 - 20.351	1.60269	18.0909 - 18.6249	00
0.90465249		19.6933 - 20.351	1.60269	18.0909 - 18.6249	14
0.90466224		19.6815 - 20.3608	1.25705	18.3292 - 18.4818	04
0.90467842		19.4215 - 20.3403	1.06968	18.2517 - 18.681	13
0.90469316		19.7238 - 20.342	1.24384	18.2606 - 18.7071	01
0.90489710	0.775974	19.6318 - 20.6485		17.6826 - 18.1864	16
0.90495529	0.539051	19.6788 - 20.6461		17.6524 - 18.224	17
0.90496564	0.593038	19.6666 - 20.1846		17.6115 - 18.4156	18
0.90496672	0.534479	19.9245 - 20.7138		17.4817 - 18.3103	15
0.90501573	0.565175	19.6303 - 20.4708		17.5776 - 18.2069	19
0.90502535	0.78465	19.6886 - 20.2024		17.6469 - 18.2795	09
0.90502799	1.8468	19.2636 - 20.6339		17.5567 - 18.5184	07
0.90509637	1.48416	19.1951 - 20.3962		17.6189 - 18.3345	06
0.90510611	0.778049	19.0163 - 20.4467		17.7317 - 18.2163	10
0.90512788	1.38257	19.4183 - 20.6451		17.6345 - 18.3804	02
0.90514017	0.957712	19.5287 - 20.4229		17.3509 - 18.566	11
0.90520394	0.965364	19.6825 - 20.2287		17.5655 - 18.5148	08
0.90648087		19.9825 - 21.1219		15.7071 - 18.2552	05

Table 2: 3D cases with 10 Ca_{40}^+ and 10 A_{80}^{2+}.

5 Real Test Case 309 Ca$_{40}^+$

6 Real Test Case 531 Ca$_{40}^+$

7 Real Test Case 2685 Ca$_{40}^+$
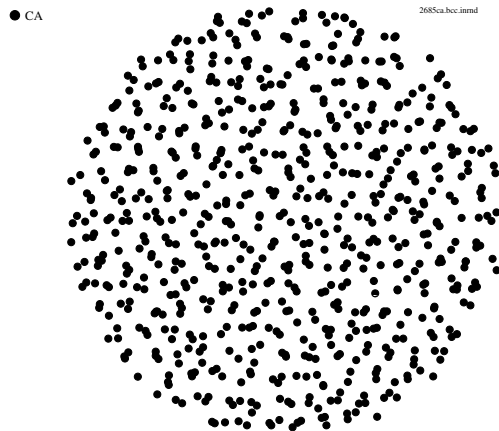
Figure 1: xyz-plane $(-20, 20)\mu m$, initial configuration with %40 pertubation.
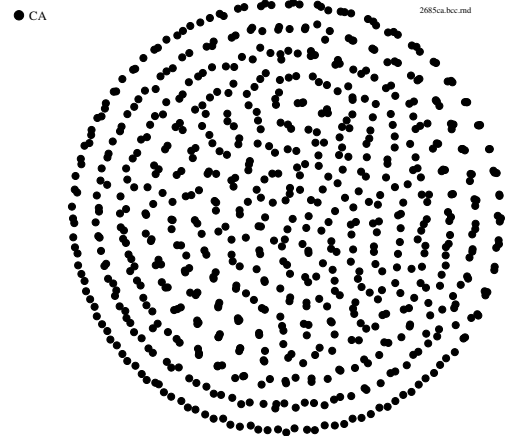
Figure 2: xyz-plane $(-20, 20)\mu m$, 3.0839[ms], $U_{\text{coh}} = -0.8919665648371$.
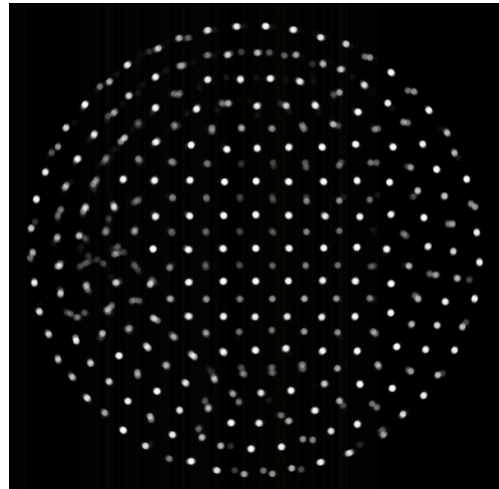

Figure 3: $1m$K, 10%.
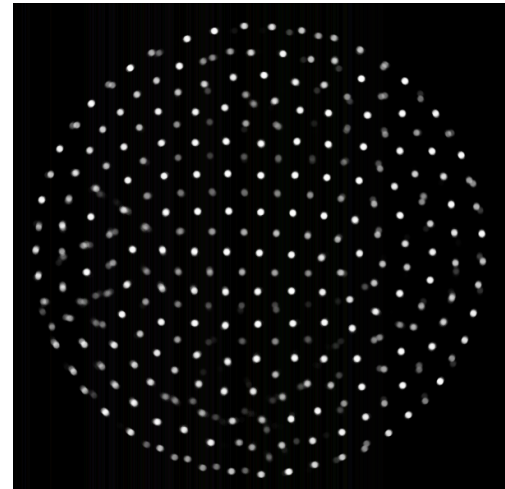
Figure 4: $1m$K, 0%.
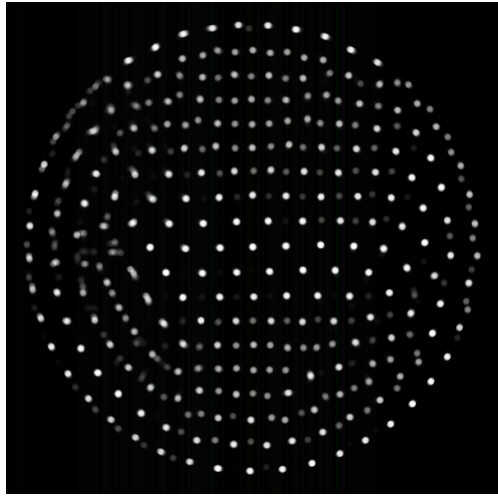
Figure 5: $1m$K, 10%, rot$(0, -40)$.
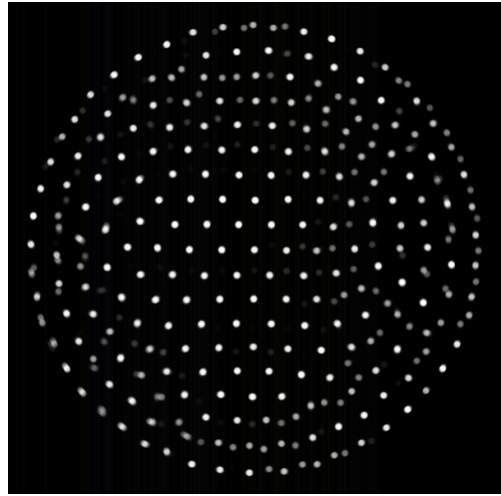
Figure 6: $1m$K, 0%, rot$(0, -40)$.
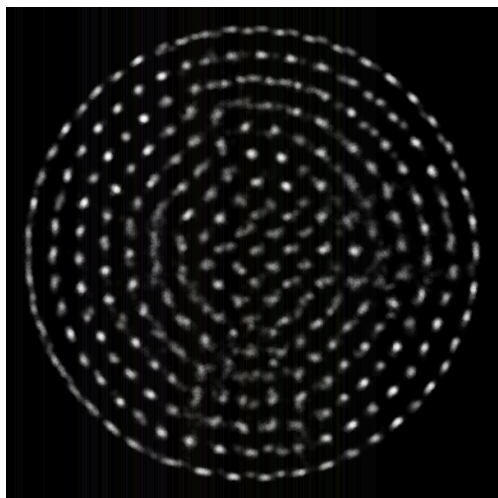

Figure 7: $5m$K, 10%.
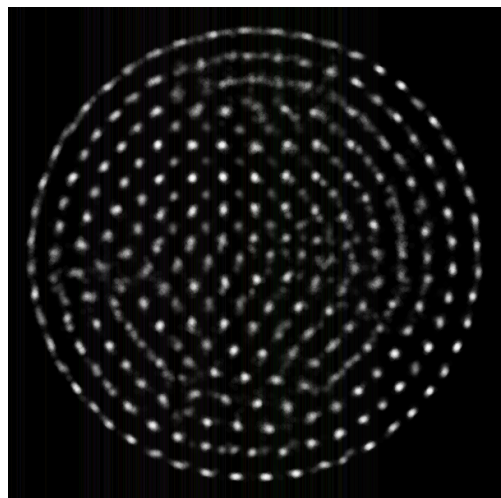
Figure 8: $5m$K, 0%.
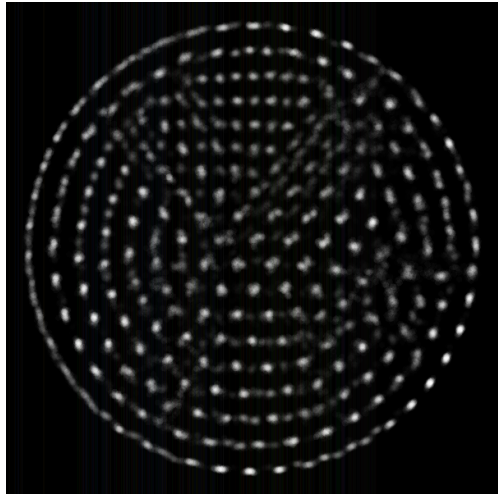
Figure 9: $5m$K, 10%, rot$(0, -40)$.
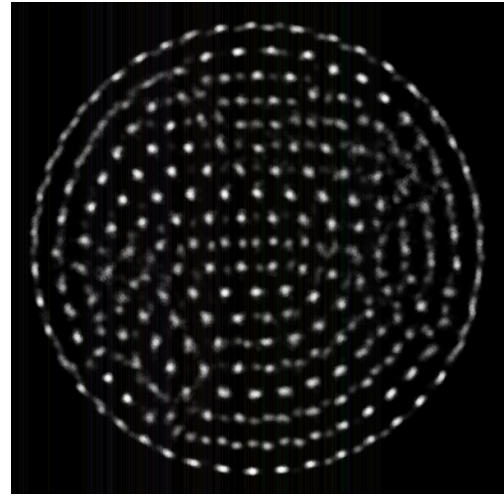
Figure 10: $5m$K, 0%, rot$(0, -40)$.
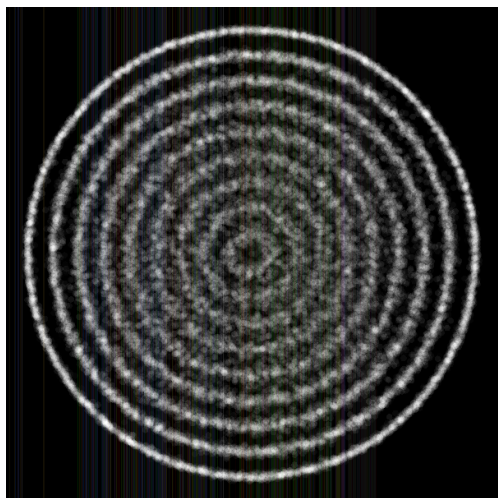
Figure 11: $10m$K, 10%.
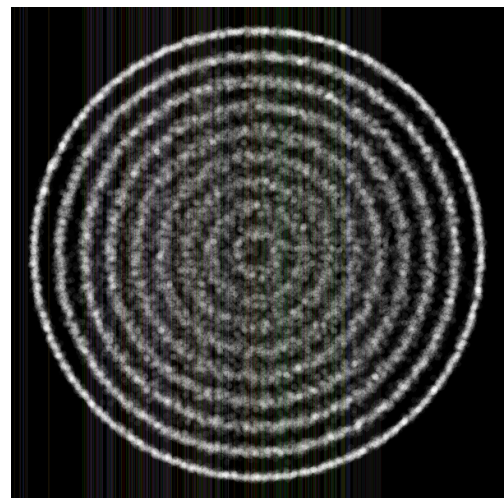
Figure 12: $10m$K, 0%.
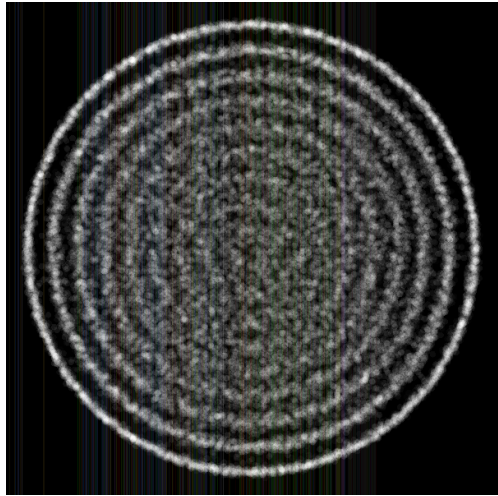
Figure 13: $15m$K, 10%.
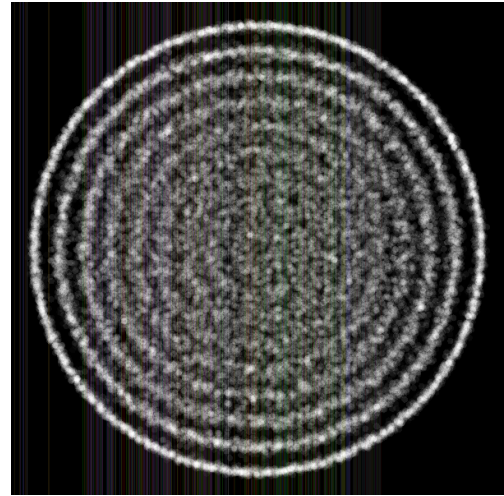
Figure 14: $15m$K, 0%.
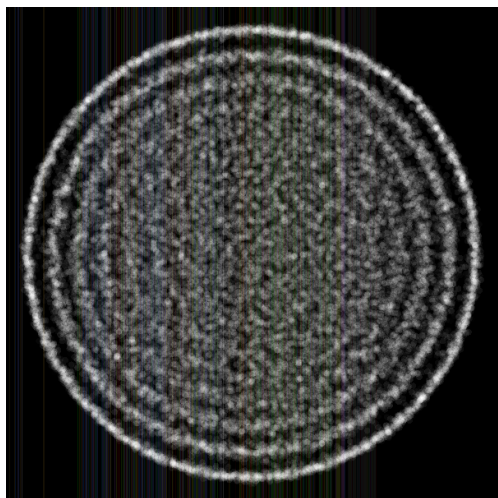
Figure 15: $20m$K, 10%.
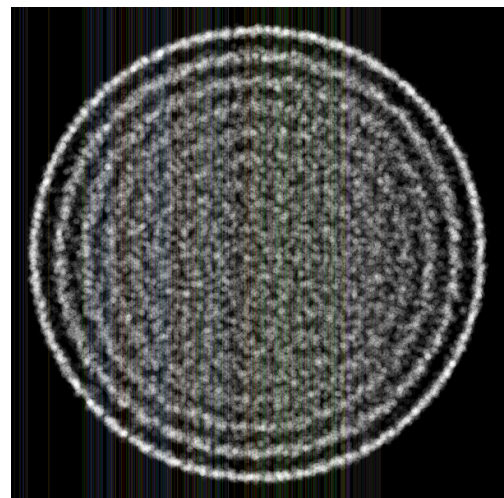
Figure 16: $20m$K, 0%.

8 Real Test Case 10179 Ca_{40}^+
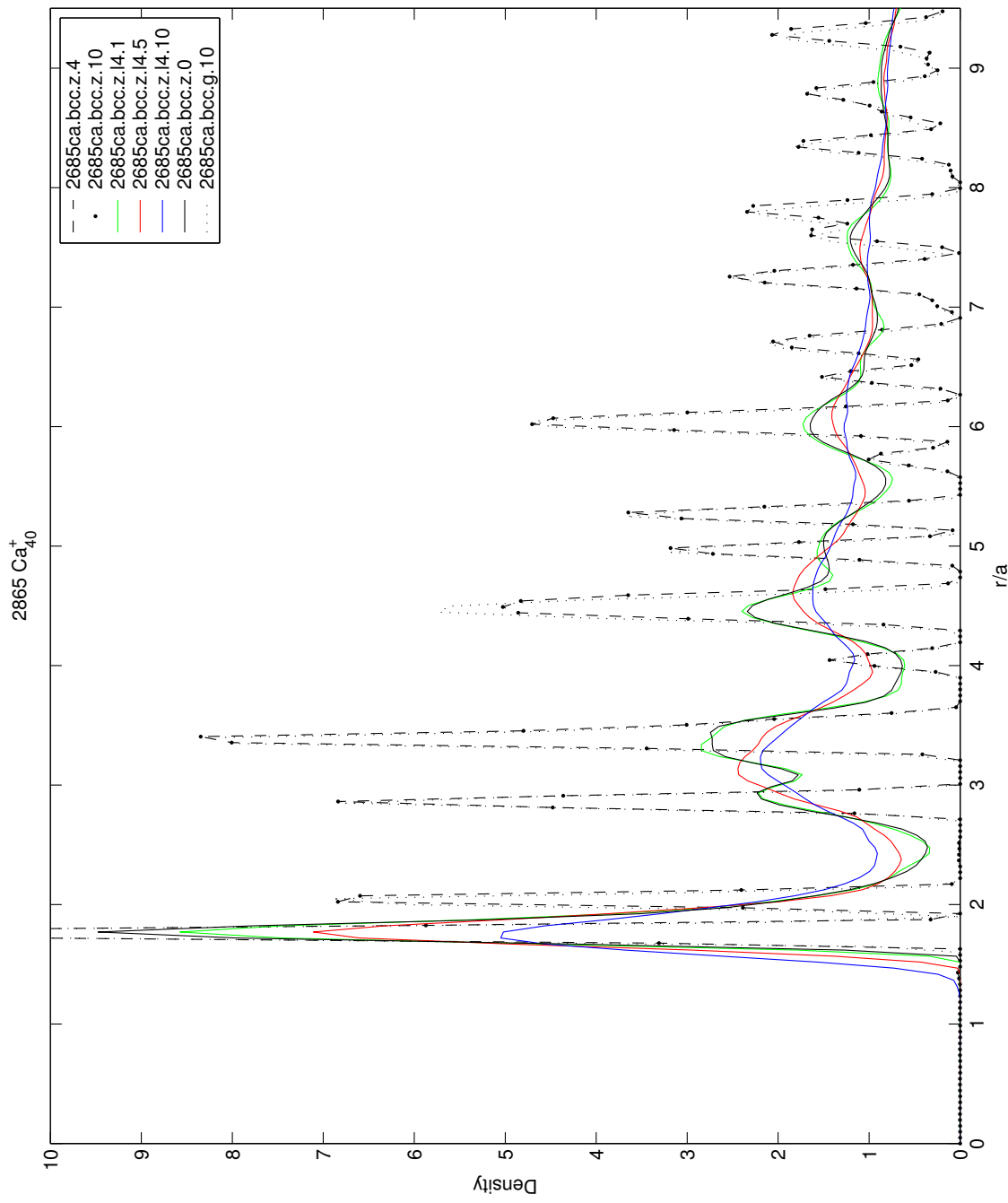
Figure 17: Radial distribution of BCC, $N = 42.4\%$, $R = 75.1\%$, 2685 Ca_{40}^{+}.
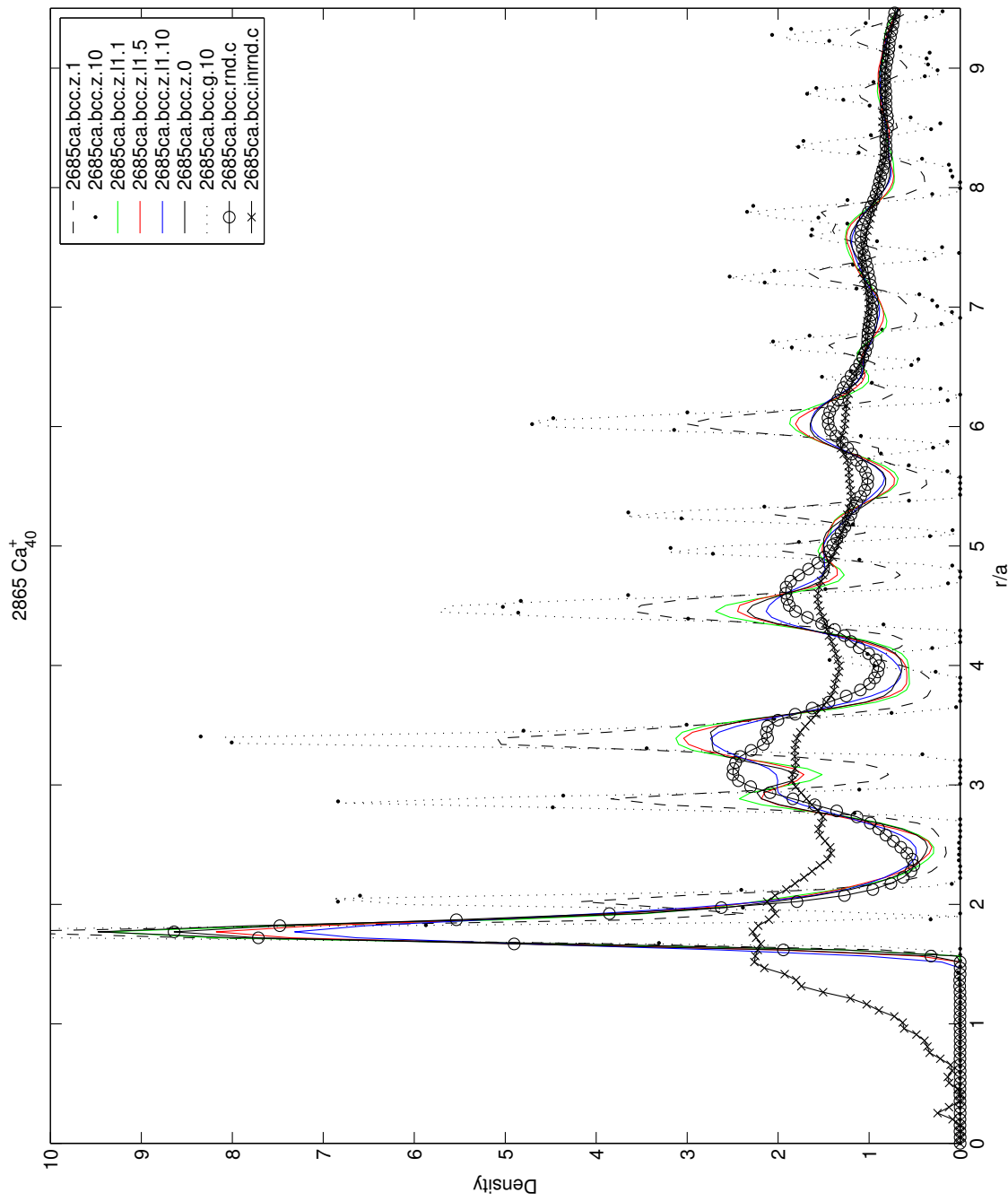
Figure 18: Radial distribution of BCC, $N = 10.5\%$, $R = 47.2\%$, 2685 Ca_{40}^{+}.
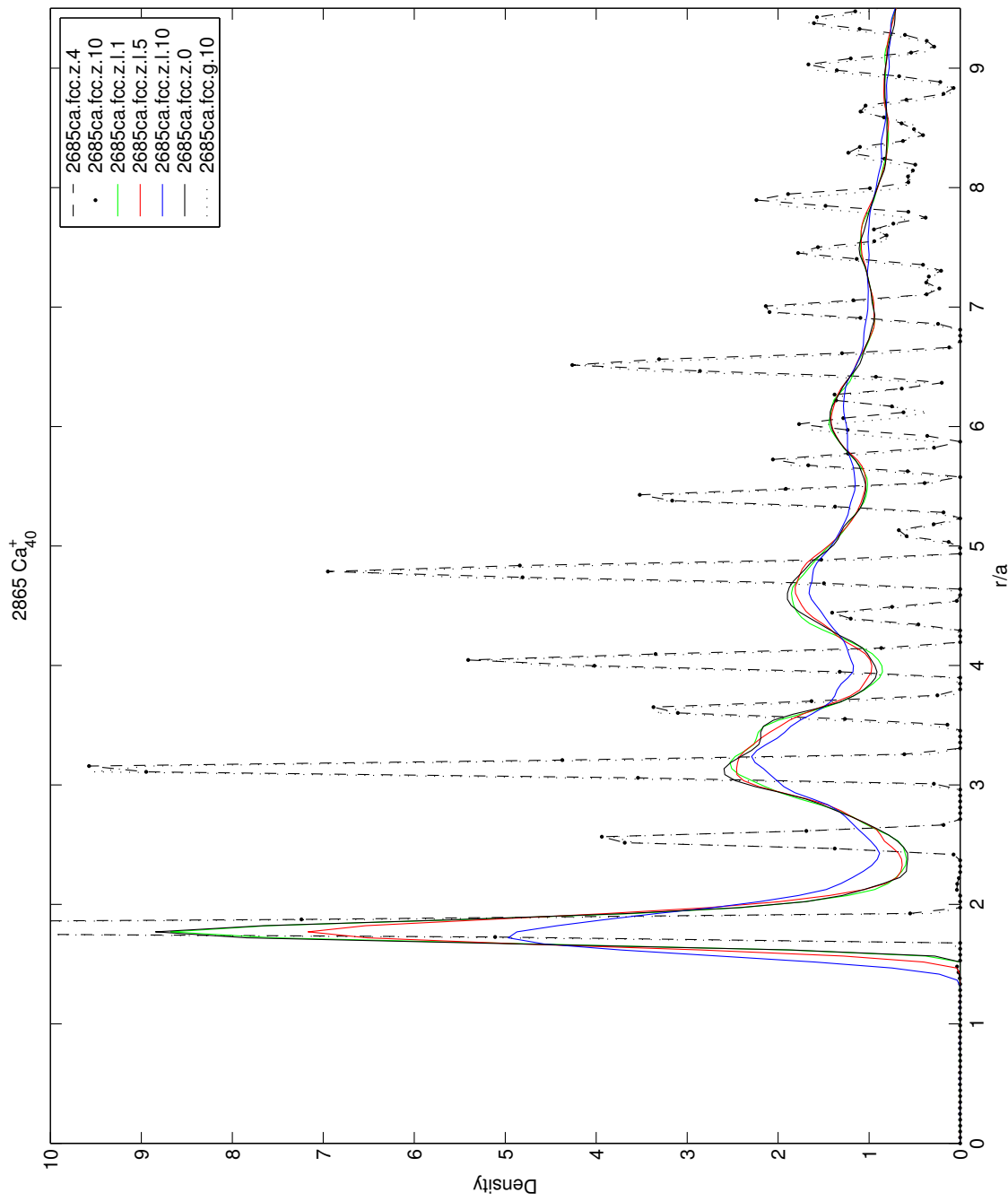
Figure 19: Radial distribution of FCC, $N = 42.4\%$, $R = 75.1\%$, 2685 Ca_{40}^+.
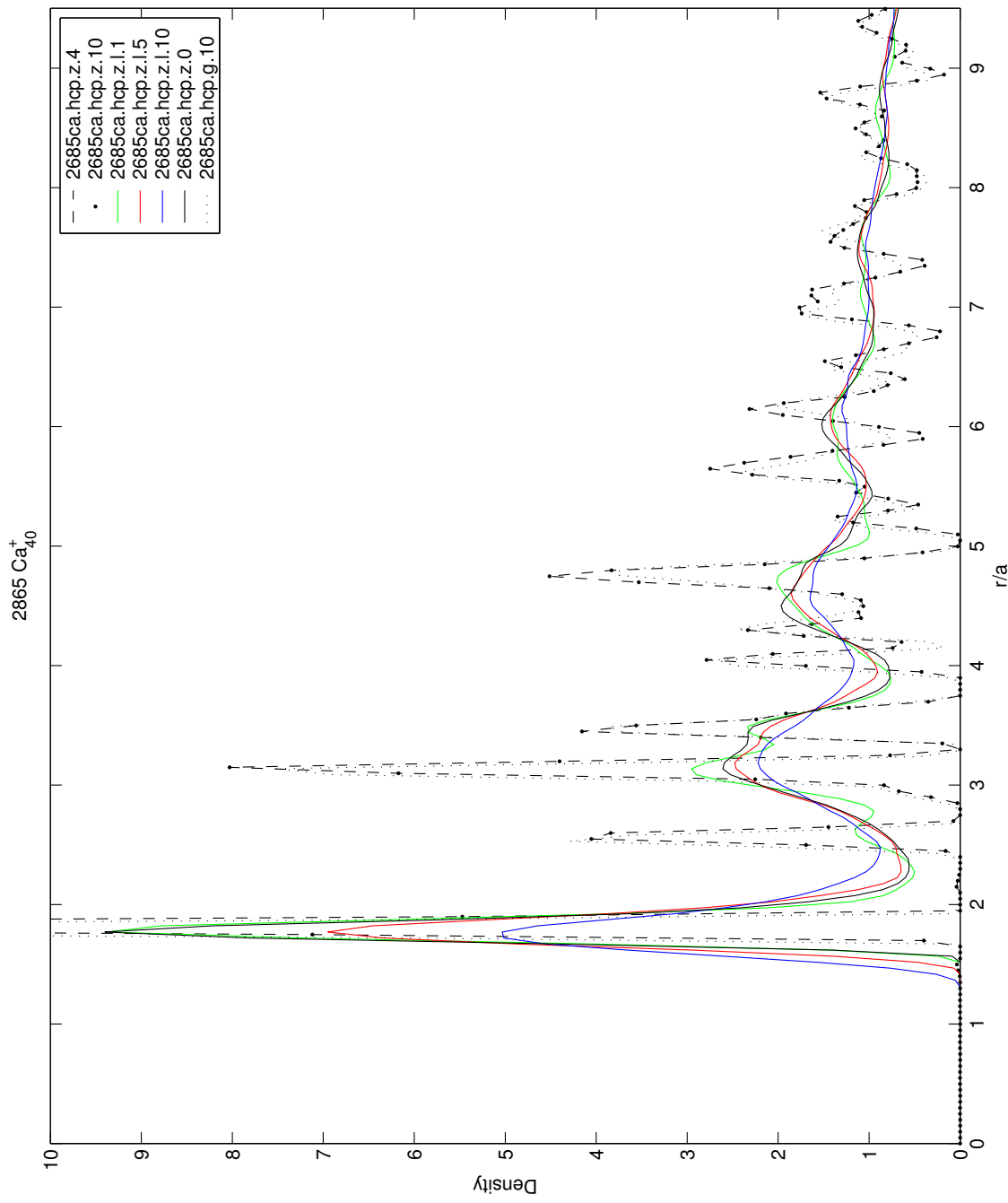
Figure 20: Radial distribution of HCP, $N = 42.4\%$, $R = 75.1\%$, 2685 Ca_{40}^+.
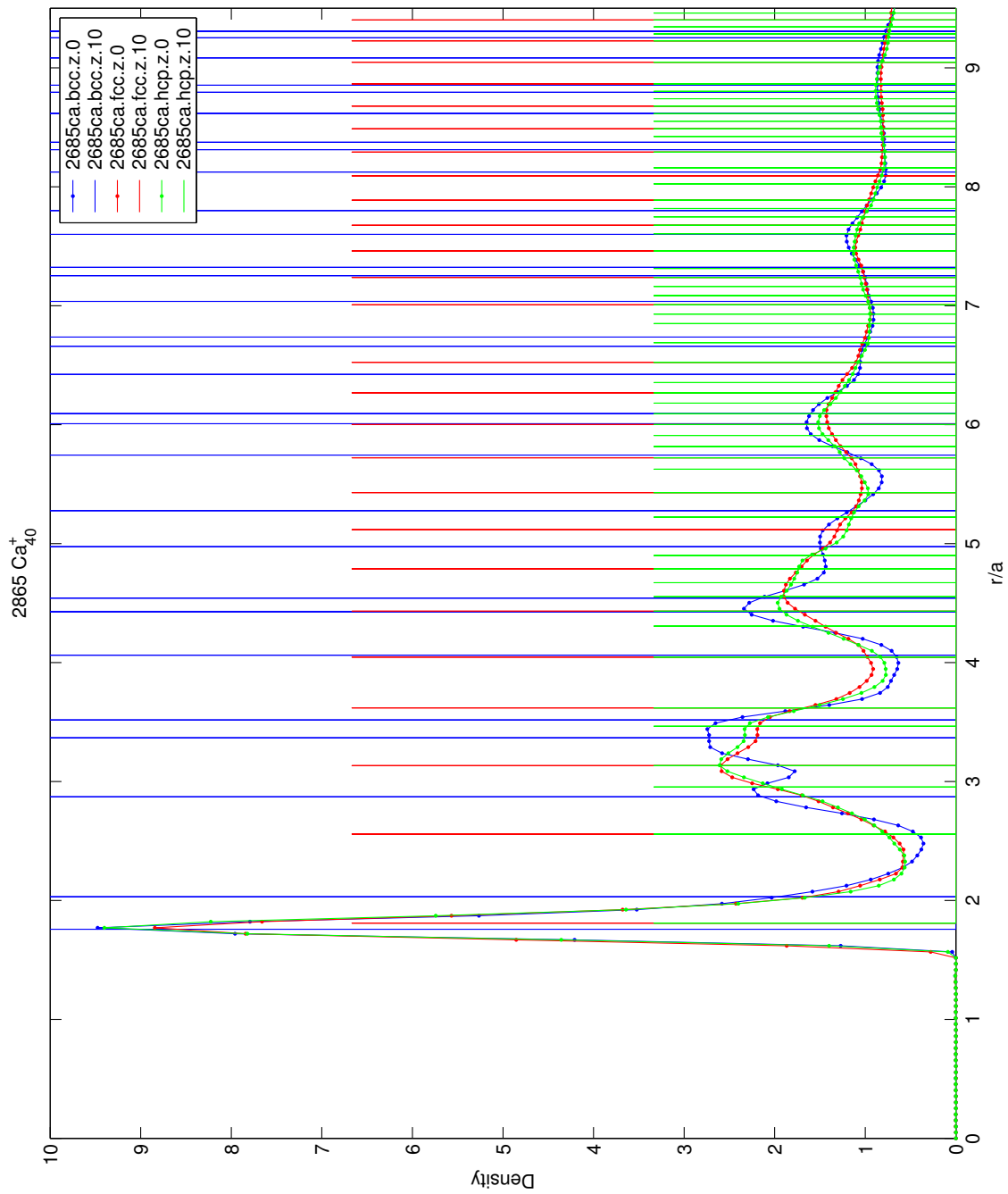
Figure 21: Radial distribution free vs. initial, 2685 Ca_{40}^{+}.
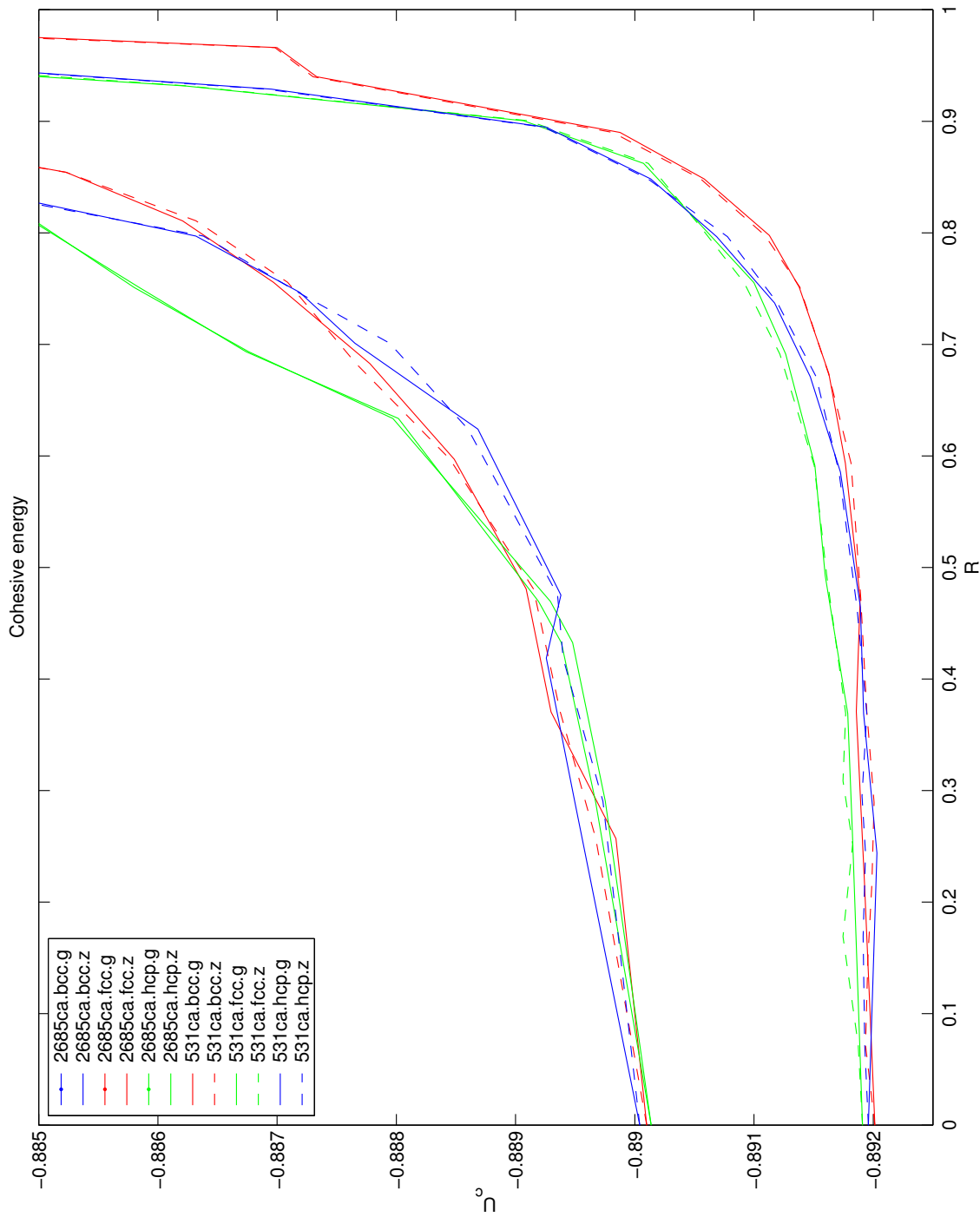
Figure 22: Cohesive energy vs. R constrained, 531 Ca_{40}^+ and 2685 Ca_{40}^+.